

Tilted wave emission in optical parametric oscillators induced by a bichromatic pumping

Stefano Longhi

Dipartimento di Fisica, Istituto Nazionale per la Fisica della Materia, Piazza Leonardo da Vinci 32, I-20133 Milano, Italy

(Received 5 January 2002; published 24 May 2002)

Tilted wave emission is found in a mean-field model of a degenerate optical parametric oscillator pumped by a bichromatic field with a frequency offset much smaller than the cavity free-spectral range. Tilted wave emission arises due to a nonadiabatic mechanism induced by the slow pump modulation, and disappears when either one of the two pump waves is blocked.

DOI: 10.1103/PhysRevE.65.057205

PACS number(s): 47.54.+r, 42.65.Sf, 42.65.Yj

The mechanism underlying pattern formation in broad-area nonlinear optical cavities, such as in lasers, optical parametric oscillators (OPOs), and Kerr cavities with injected signal, is usually dictated by a rather simple geometric rule by means of which diffractive tilted waves can fit the cavity resonance allowing maximum energy extraction from the medium (see, e.g., [1–8]). In mean-field models, the transverse wave-number k_c of the patterns scales like $k_c \sim \sqrt{-\theta}$, where $\theta \equiv \omega_c - \omega$ is the cavity detuning parameter that measures the distance of the longitudinal frequency ω_c of the cavity from the excitation frequency ω . Pattern formation is thus prevented for a positive detuning parameter, $\theta > 0$. A rather distinct mechanism for pattern formation may occur when the dynamics of the system becomes nonautonomous and involves at least two scalar wave fields. Such a mechanism has been recently identified and studied for OPO and laser systems by allowing the cavity detuning parameter θ to periodically and slowly vary in time [9,10]. In this case, it was shown that, even on the positive detuning side of cavity resonance, i.e., for $\theta(t) > 0$ at any time, pattern formation becomes possible. The effect of cavity detuning modulation is to bring the system periodically from above to below threshold, i.e., the instantaneous growth rate of perturbations is periodically swept from positive to negative values. Owing to the two-field dynamics, in the temporal windows where the instantaneous growth rate is negative, the damping is not monotonic, instead damped coherent oscillations occur at a frequency that depends on the transverse wave number of perturbation. The overall growth rate of transverse perturbations over one modulation cycle is largely influenced by the existence of such coherent oscillations, and it may happen that a perturbation with a nonzero wave number is favored despite its instantaneous growth rate is not the highest. This mechanism for pattern formation was referred to as *nonadiabatic* since it disappears when the modulation is either too fast or too slow as compared to the typical time scale of the system. Owing to the rather generic nature of such a mechanism, one can expect nonadiabatic tilted wave emission to occur whenever the autonomous dynamics of the system is broken, not necessarily by modulation of cavity detuning [11].

In this Brief Report, we present another example of nonadiabatic tilted wave emission by considering a degenerate OPO subjected to a bichromatic pumping [11]. We consider the mean-field model of a broad-area doubly resonant degenerate OPO with flat end mirrors that converts a not-resonated

nearly monochromatic plane-wave pump field at frequency 2ω into degenerate signal and idler waves at frequency ω (Fig. 1). We assume that the pump wave is bichromatic, comprising two spectral components at frequencies $2\omega \pm \Omega$ (see Fig. 1). Assuming a frequency separation 2Ω of the two pump waves much smaller than the cavity free-spectral range and of the order of the cavity linewidth, a mean-field equation describing the dynamics of the normalized amplitude A of intracavity signal field at frequency ω can be derived using the same technique as detailed in Ref. [12]. In the paraxial approximation and assuming perfect phase matching in the nonlinear $\chi^{(2)}$ crystal, the mean-field equation reads

$$\partial_t A = -(\gamma + i\theta)A + \mu(t)A^* + ia\nabla^2 A - |A|^2 A, \quad (1)$$

where γ is the cavity decay rate for the signal field; $\theta = (\omega_c - \omega)$ is the detuning parameter that provides the distance of the nearest longitudinal cavity resonance ω_c from ω ; $\nabla^2 = \partial_x^2 + \partial_y^2$ is the transverse Laplacian; a is the diffraction parameter; and

$$\mu(t) = \mu_1 \exp(i\Omega t) + \mu_2 \exp(-i\Omega t) \quad (2)$$

is the parametric gain, where μ_1 and μ_2 are proportional to the amplitudes of the external pump waves at frequencies $2\omega - \Omega$ and $2\omega + \Omega$, respectively. Let us notice that, in case of a single monochromatic wave pumping the crystal, i.e., for $\mu_1 = 0$ or $\mu_2 = 0$, Eq. (1) can be cast in an autonomous form by the substitution $A = B \exp(\pm i\Omega t/2)$, yielding

$$\partial_t B = -\left(\gamma + i\theta \pm i\frac{\Omega}{2}\right)B + \mu_{1,2}B^* + ia\nabla^2 B - |B|^2 B. \quad (3)$$

Equation (3) describes in the usual form the parametric down conversion process of pump photons at frequency $2\omega \mp \Omega$ into photons at frequency $\omega \mp \Omega/2$, with an effective detuning parameter given by $\theta_{1,2} \equiv \theta \pm \Omega/2$. In this case, it is known that a pattern forming instability sets in at the OPO threshold through a tilted wave mechanism whenever the effective detuning parameter $\theta_{1,2}$ is negative [4]. Notice that if θ is positive and $\Omega < 2\theta$, both $\theta_{1,2}$ are positive, and pattern

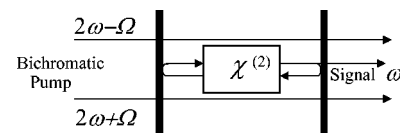


FIG. 1. Schematic of a doubly resonant degenerate OPO with a bichromatic pump.

formation is hence prevented if either one of the two pump waves is blocked. Let us now consider the case where the two pump waves are *simultaneously* incident into the crystal. In this case, Eq. (1) is strictly nonautonomous, with coefficients that are periodic with period $T=2\pi/\Omega$. The stability analysis of the zero solution $A=0$ and the onset of parametric instability can be performed in this case using Floquet theory following an analysis similar to that given in Refs. [9,10]. For the sake of simplicity, we assume that the pump waves have the same amplitude, e.g., that $|\mu_1|=|\mu_2|\equiv\mu_0/2$, and we take μ_0 as the bifurcation parameter in Eq. (1). Moreover, after a suitable redefinition of the phase of A and a time translation, one may set in Eq. (1) $\mu(t)=\mu_0\cos(\Omega t)$. The bichromatic pumping thus realizes a slow modulation, at a frequency Ω , of the amplitude of the parametric gain. To investigate the linear stability of the trivial zero solution $A=0$, that corresponds to the OPO being below threshold, let us set $A=A_1\exp(-\gamma t+i\mathbf{k}\cdot\mathbf{r})+A_2^*\exp(-\gamma t-i\mathbf{k}\cdot\mathbf{r})$, where \mathbf{k} is the wave vector of the perturbation and $\mathbf{r}=(x,y)$ contains the transverse spatial variables. The small amplitudes $A_{1,2}$ of perturbation satisfy the following linearized equations:

$$\frac{dA_1}{dt}=i\theta_k A_1+\mu(t)A_2, \quad (4)$$

$$\frac{dA_2}{dt}=-i\theta_k A_2+\mu(t)A_1, \quad (5)$$

where $\theta_k\equiv-(ak^2+\theta)$ and $k\equiv|\mathbf{k}|$. The solution to Eqs. (4) and (5) in one period can be cast in the matrix form $[A_1(T),A_2(T)]^T=M[A_1(0),A_2(0)]^T$, where the coefficients of the 2×2 matrix M satisfy the relations $M_{22}=M_{11}^*$ and $M_{21}=M_{12}^*$. If $\sigma_{\pm}=\sigma_{\pm}(\mu_0,k)$ are the eigenvalues of the matrix M , according to Floquet theory an instability for the perturbation with wave-number k occurs whenever

$$|\sigma_{\pm}|\geq\exp(\gamma T) \quad (6)$$

for either one of the two eigenvalues. By taking the equality in Eq. (6), we obtain the neutral stability curve $\mu_0=\mu_0(k)$ for the instability of the perturbation with wave-number k . The threshold for parametric oscillation is then given by $\mu_{th}=\min_k\mu_0(k)=\mu_0(k_c)$ with critical wave-number k_c . We note that, owing to the relations among the matrix coefficients, one has $\sigma_{\pm}=\text{Re}(M_{11})\pm\{[\text{Re}(M_{11})^2-1]\}^{1/2}$, so that the determination of the instability condition requires the knowledge of the matrix coefficient M_{11} solely. The calculation of M_{11} can be obtained by numerical integration of Eqs. (4) and (5) in one period with the initial condition $[A_1(0),A_2(0)]^T=(1,0)$, so that $M_{11}=A_1(T)$. In Fig. 2, the main results of the linear stability analysis are reported, showing the behavior of the OPO threshold [Fig. 2(a)] and of the critical wave-number k_c versus frequency Ω [Fig. 2(b)] for $\theta=1$ and $\gamma=0.1$. In Fig. 2(a), the behavior of the instability boundary for the zero mode ($k=0$) is also reported for comparison. A pattern forming instability, corresponding to a nonvanishing critical wave number, is observed for $\Omega>2\theta$ and in a sequence of frequency intervals for $\Omega<2\theta$ that

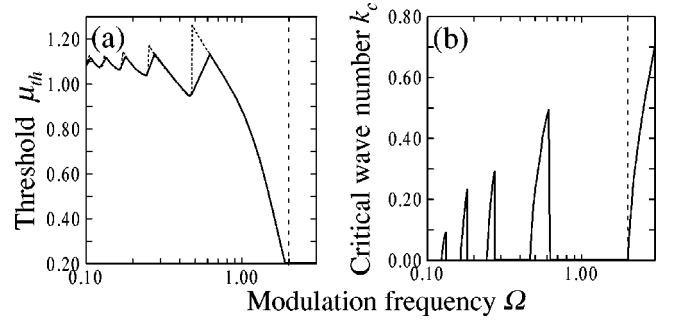


FIG. 2. (a) Threshold μ_{th} for parametric oscillation (solid curve), and (b) corresponding critical wave-number k_c as a function of frequency offset Ω . The dashed curve in (a), partially overlapped with the solid one, is the threshold for parametric oscillation in the plane-wave limit ($k=0$). The vertical dashed lines in (a) and (b) correspond to the abscissa $\Omega=2\theta$. For $\Omega>2\theta$, the solid curve in (b) is overlapped with the curve $k_c=[(\Omega/2-\theta)/a]^{1/2}$. Parameter values are: $a=1$, $\theta=1$, and $\gamma=0.1$.

become narrower as they accumulate toward $\Omega\rightarrow 0$. Typical examples of neutral stability curves with a nonvanishing critical wave number for $\Omega<2\theta$ and $\Omega>2\theta$ are shown in Fig. 3. For $\Omega<2\theta$, the existence of frequency intervals where off-axis emission occurs is a signature of the nonautonomous dynamics induced by the interference of the two pump waves: stopping either one of the two pump waves would in fact prevent off-axis emission. The tendency of the system to emit off-axis waves for $\Omega<2\theta$ is related to the existence of coherent field oscillations when $|\mu(t)|$ becomes smaller than θ , which may largely influence the overall growth rate of the perturbation over one modulation cycle. Such a phenomenon is analogous to that found in the case of modulation of detuning θ and constant parametric gain μ , which was extensively discussed in Refs. [9,10]. For $\Omega<2\theta$, the qualitative behavior of OPO threshold and critical wave number versus frequency Ω , shown in shown in Figs. 2(a) and 2(b), is indeed fully analogous to that found in the case of modulation of detuning (see, e.g., Fig. 1 of Ref. [9]). In particular, the asymptotic value of the threshold for $\Omega\rightarrow 0$ is found by the condition that the average growth rate of perturbation due to the parametric gain in one modulation cycle equals the loss rate, that is

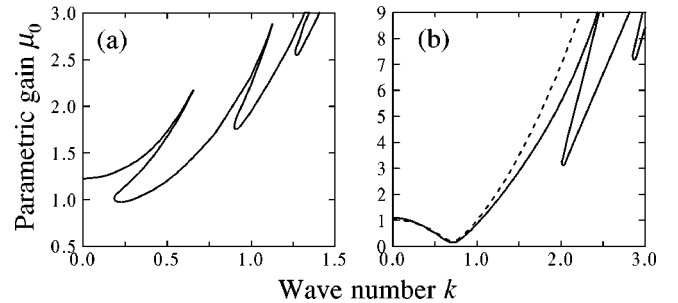


FIG. 3. Neutral stability curve for (a) $\Omega=0.5$ and (b) $\Omega=3$. The other parameter values are the same as in Fig. 2. In (b), the dashed line is the behavior of the neutral stability that one would obtain by stopping the pump beam at frequency $2\omega-\Omega$ [Eq. (8) in the text].

$$\text{Re} \left[\frac{1}{T} \int_0^T \sqrt{\mu_{ih}^2 \cos^2(\Omega t) - \theta^2} \right] = \gamma. \quad (7)$$

A notable difference as compared to the case of modulation of detuning is the absence of a cutoff frequency above which off-axis emission is prevented. In the case of modulation of cavity detuning $\theta = \theta(t)$ and constant pumping μ , the existence of a cutoff frequency is due to the fact that, for a fast modulation, one can replace $\theta(t)$ by its time average in the mean-field equation [9]. Conversely, in the case of modulation of the parametric gain μ with constant detuning θ , for $\Omega > 2\theta$ a threshold lowering to 2γ is observed, corresponding to off-axis emission with a critical wave-number k_c that is well approximated by the geometric tilted wave rule $k_c = [(\Omega/2 - \theta)/a]^{1/2}$ with an effective detuning given by $\theta_1 = \theta - \Omega/2$ (see Fig. 2). This circumstance is related to the fact that, for $\Omega > 2\theta$, the pump wave at frequency $2\omega + \Omega$ can resonantly excite off-axis waves with wave-number k_c [see Eq. (3)], and at leading order one can disregard the effect of the other pump wave. Indeed, Fig. 3(b) shows that, for $\Omega > 2\theta$, the neutral stability curve obtained by the rigorous Floquet analysis can be well approximated, at least near the critical wave-number k_c , by the one obtained by disregarding the effect of the pump wave at frequency $2\omega - \Omega$, i.e., by the curve

$$\mu_0(k) = 2\sqrt{\gamma^2 + (ak^2 + \theta - \Omega/2)^2}. \quad (8)$$

Above the linear instability, a set of amplitude equations of standard Landau form with cubic terms solely can be derived near threshold to describe the competition of neutral modes on the critical circle $k = k_c$ using the same technique as detailed in Refs. [9,10]. As it was shown in those references, though the nonautonomous dynamics strongly affect the neutral stability curve allowing for off-axis wave emission, it has no appreciable effect on the nonlinearity of the system, which rules out the pattern selection mechanism. For Eq. (1), amplitude equations predict the formation of roll patterns due to the fact that cross saturation dominates over self saturation in the nonlinear cubic terms [9]. The prediction of nonadiabatic pattern formation provided by the linear stability analysis has been confirmed by a direct numerical analysis of Eq. (1) in two-transverse spatial dimensions using a standard split-step pseudospectral technique with periodic boundary conditions. Numerical simulations indicate off-axis emission in the far field with the formation of roll-dominated patterns with the calculated transverse wave vector in the

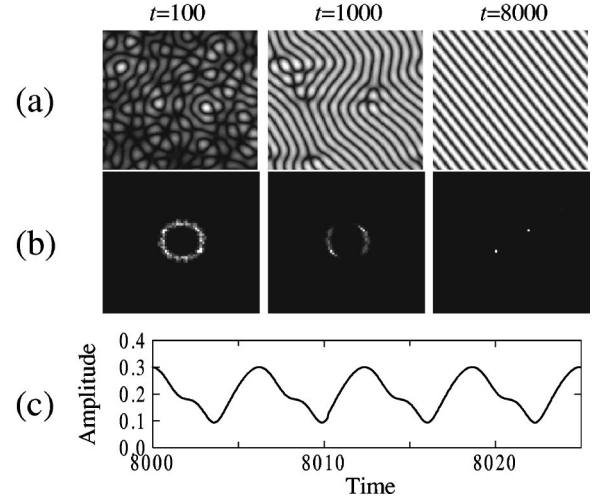


FIG. 4. Snapshots of near-field (a) and far-field (b) spatial intensity profiles of signal field at successive times showing the formation of roll patterns starting from a small random noise. Parameter values are the same as in Fig. 3(a). The parametric gain is $\mu_0 = 1.1$. In (c) are shown the oscillations of the roll amplitude over a few modulation cycles. The computation window is a square of size 82×82 on a 128×128 spatial grid; time step: $dt = 0.01$.

near field. A typical example of off-axis wave emission, corresponding to the parameter values of Fig. 3(a), is shown in Fig. 4. Notice that a fast periodic modulation of roll amplitude occurs on the time scale of the external modulation [see Fig. 4(c)]. As a final remark, we note that the phenomenon of off-axis wave emission induced by a bichromatic pumping is not restricted to the degenerate OPO configuration studied in this Brief Report, but it can be observed analogously in a nondegenerate OPO model [10].

In conclusion, we have presented a nonadiabatic mechanism for pattern formation in a doubly resonant degenerate optical parametric oscillator pumped by a bichromatic field. Off-axis emission is sustained by the coherent dynamics that occurs due to the slow modulation of the parametric gain and disappears when either one of the two pumping beams is stopped. Analogies and differences with off-axis wave emission previously studied in case of modulation of cavity detuning have been pointed out. We envisage that the bichromatic pumping scheme proposed in this Brief Report may be more accessible than cavity length modulation for an experimental observation of nonadiabatic pattern formation processes and may help in dissipating any suspicion that might be hidden in the interpretation of such processes [11].

- [1] P.K. Jakobsen, J.V. Moloney, A.C. Newell, and R. Indik, Phys. Rev. A **45**, 8129 (1992); Q. Feng, J.V. Moloney, and A.C. Newell, Phys. Rev. Lett. **71**, 1705 (1993).
 [2] A.C. Newell and J.V. Moloney, *Nonlinear Optics* (Addison-Wesley, Redwood City, CA, 1992).
 [3] W.J. Firth and A.J. Scroggie, Europhys. Lett. **26**, 521 (1994).
 [4] G.-L. Oppo, M. Brambilla, and L.A. Lugiato, Phys. Rev. A **49**, 2028 (1994).

- [5] K. Staliunas, J. Mod. Opt. **42**, 1261 (1995).
 [6] G.J. de Valcarcel, K. Staliunas, E. Roldan, and V.J. Sanchez-Morcillo, Phys. Rev. A **54**, 1609 (1996).
 [7] L.A. Lugiato, M. Brambilla, and A. Gatti, in *Optical Pattern Formation*, Advances in Atomic, Molecular and Optical Physics, Vol. 40, edited by B. Bedersen and H. Walther (Academic Press, Boston, 1998).
 [8] U. Bortolozzo, P. Villoresi, and P.L. Ramazza, Phys. Rev. Lett.

87, 274102 (2001).

[9] S. Longhi, Phys. Rev. Lett. **84**, 5756 (2000).

[10] S. Longhi, Phys. Rev. A **63**, 023808 (2001).

[11] We note that, in the case of modulation of detuning $\theta = \theta(t)$ considered in Refs. [9,10], the longitudinal cavity mode of the lossless empty cavity is not a monochromatic wave at frequency ω_c , instead its spectrum shows sideband modes at frequencies $\omega_c \pm n\Omega$, where Ω is the modulation frequency and $n = 0, \pm 1, \pm 2, \dots$, [see, e.g., G.T. Moore, J. Math. Phys. **1**, 2679 (1970); V.V. Dodonov, A.B. Klimov, and V.I. Man'ko, Phys. Lett. A **149**, 225 (1990)]. As an example, for a sinusoidal modulation of cavity detuning around a mean value θ_0 with a modulation depth δ , $\theta(t) = \theta_0 + \delta \cos(\Omega t)$, the amplitude of

the sideband spectral mode of order n is given by the Bessel function $J_n(\delta/\Omega)$. In this case one might be suspicious that off-axis wave emission predicted by the linear stability analysis could be in a certain sense traced back to the usual geometric tilted wave mechanism involving the spectral sideband modes at frequencies *lower* than the excitation frequency ω , belittling the interpretation based on coherent effects discussed in Refs. [9,10]. Though this is not the case, the study of a nonadiabatic mechanism for pattern formation that does not involve any modulation of cavity length, as given in this Brief Report, seems of major importance in dissipating any possible misinterpretation underlying pattern formation in nonautonomous systems.

[12] S. Longhi, J. Mod. Opt. **43**, 1089 (1996).